



OPEN ACCESS

EDITED BY

Don J. Diamond,
City of Hope National Medical Center,
United States

REVIEWED BY

Facundo Fiocca Vernengo,
Charité Medical University of Berlin, Germany
Denise Cecil,
University of Washington, United States

*CORRESPONDENCE

Olivera J. Finn

✉ ojfinn@pitt.edu

Panayiotis V. Benos

✉ pbenos@ufl.edu

Mark J. Cameron

✉ mjc230@case.edu

†These authors have contributed equally to
this work

RECEIVED 23 May 2024

ACCEPTED 23 September 2024

PUBLISHED 10 October 2024

CITATION

Cameron CM, Raghu V, Richardson B,
Zagore LL, Tamilselvan B, Golden J,
Cartwright M, Schoen RE, Finn OJ, Benos PV
and Cameron MJ (2024) Pre-vaccination
transcriptomic profiles of immune responders
to the MUC1 peptide vaccine for colon
cancer prevention.

Front. Immunol. 15:1437391.

doi: 10.3389/fimmu.2024.1437391

COPYRIGHT

© 2024 Cameron, Raghu, Richardson, Zagore,
Tamilselvan, Golden, Cartwright, Schoen, Finn,
Benos and Cameron. This is an open-access
article distributed under the terms of the
[Creative Commons Attribution License \(CC BY\)](https://creativecommons.org/licenses/by/4.0/).
The use, distribution or reproduction in other
forums is permitted, provided the original
author(s) and the copyright owner(s) are
credited and that the original publication in
this journal is cited, in accordance with
accepted academic practice. No use,
distribution or reproduction is permitted
which does not comply with these terms.

Pre-vaccination transcriptomic profiles of immune responders to the MUC1 peptide vaccine for colon cancer prevention

Cheryl M. Cameron^{1†}, Vineet Raghu^{2,3†}, Brian Richardson^{1,4†},
Leah L. Zagore⁴, Banumathi Tamilselvan¹, Jackelyn Golden⁴,
Michael Cartwright⁴, Robert E. Schoen⁵, Olivera J. Finn^{6*},
Panayiotis V. Benos^{7,8*} and Mark J. Cameron^{4*}

¹Department of Nutrition, Case Western Reserve University, Cleveland, OH, United States, ²Department of Computer Science, University of Pittsburgh, Pittsburgh, PA, United States, ³Massachusetts General Hospital, Harvard Medical School, Cambridge, MA, United States, ⁴Department of Population and Quantitative Health Sciences, Case Western Reserve University, Cleveland, OH, United States, ⁵Division of Gastroenterology, Hepatology and Nutrition, University of Pittsburgh, Pittsburgh, PA, United States, ⁶Department of Immunology, University of Pittsburgh, Pittsburgh, PA, United States, ⁷Department of Epidemiology, University of Florida, Gainesville, FL, United States, ⁸Department of Computational and Systems Biology, University of Pittsburgh, Pittsburgh, PA, United States

Introduction: Self-antigens abnormally expressed on tumors, such as MUC1, have been targeted by therapeutic cancer vaccines. We recently assessed in two clinical trials in a preventative setting whether immunity induced with a MUC1 peptide vaccine could reduce high colon cancer risk in individuals with a history of premalignant colon adenomas. In both trials, there were immune responders and non-responders to the vaccine.

Methods: Here we used PBMC pre-vaccination and 2 weeks after the first vaccine of responders and non-responders selected from both trials to identify early biomarkers of immune response involved in long-term memory generation and prevention of adenoma recurrence. We performed flow cytometry, phosflow, and differential gene expression analyses on PBMCs collected from MUC1 vaccine responders and non-responders pre-vaccination and two weeks after the first of three vaccine doses.

Results: MUC1 vaccine responders had higher frequencies of CD4 cells pre-vaccination, increased expression of CD40L on CD8 and CD4 T-cells, and a greater increase in ICOS expression on CD8 T-cells. Differential gene expression analysis revealed that iCOSL, PI3K AKT MTOR, and B-cell signaling pathways are activated early in response to the MUC1 vaccine. We identified six specific transcripts involved in elevated antigen presentation, B-cell activation, and NF- κ B1 activation that were directly linked to finding antibody response at week 12. Finally, a model using these transcripts was able to predict non-responders with accuracy.

Discussion: These findings suggest that individuals who can be predicted to respond to the MUC1 vaccine, and potentially other vaccines, have greater readiness in all immune compartments to present and respond to antigens. Predictive biomarkers of MUC1 vaccine response may lead to more effective vaccines tailored to individuals with high risk for cancer but with varying immune fitness.

KEYWORDS

colon cancer, colorectal adenoma, cancer vaccine, transcriptomics, MUC1, serological response

Introduction

Self-antigens abnormally expressed in tumors, known as non-viral cancer-associated antigens, have been extensively tested over the last three decades as antigens in therapeutic cancer vaccines (1–3). In preclinical studies, an immune response to these antigens can prevent cancer growth without causing toxicity. In humans, preexisting immunity to some such antigens correlates with better disease outcome or reduced risk of cancer recurrence (4). Nevertheless, therapeutic vaccines utilizing these antigens have had low immunogenicity and no clinical efficacy. This has been attributed to the presence of many immunosuppressive factors in the tumor microenvironment, such as regulatory T cells (Tregs), myeloid-derived suppressor cells (MDSCs), and tumor associated macrophages (TAMs), all of which actively suppress the activity of cytotoxic T cells and other immune effector cells. Additionally, the secretion of immunosuppressive cytokines like IL-10 and TGF- β , along with expression of immune checkpoint molecules such as PD-L1, further exacerbates immune suppression leading to an antagonistic environment for antitumor immune responses (5–7).

MUC1 is a cancer-associated antigen that has been effective as a vaccine in preclinical animal models but showed limited immunogenicity and efficacy as a therapeutic vaccine in clinical trials in colon, breast, pancreas, prostate and lung cancer (8–12). Hypothesizing that the major difference between the outcome of the vaccine in preclinical models and clinical trials is the high level of immune suppression in cancer patients, we began to develop models and MUC1 vaccines for cancer prevention in patients at risk; before immune suppression develops. As MUC1 is expressed on early premalignant lesions as well as cancer, we chose to study immunogenicity, safety and potential efficacy of this vaccine in the preventative setting in individuals with a history of colonic polyps that increases their risk of colon cancer (13).

From 2008 to 2012, we conducted a single arm trial (NCT-007773097) in 41 individuals (14). Participants received a vaccine comprised of a 100-amino acid synthetic MUC1 protein (100 μ g), admixed with the adjuvant polyinosinic-polycytidylic acid (Poly ICLC – Hiltonol), a synthetic dsRNA analog and Toll-like receptor

3 (TLR3) agonist (14). The vaccine was administered subcutaneously at week 0, 2, and 10, with a booster dose given at week 52. Forty-three percent (43%) of vaccinated participants responded to the vaccine as measured by production of anti-MUC1 IgG at week 12 post vaccination (vaccine responders), and 57% did not respond (vaccine non-responders). From 2015–2020, we conducted the second study, a randomized, double-blind placebo-controlled multi-center efficacy trial of the same MUC1 vaccine in the setting of newly diagnosed advanced adenomas in 110 individuals (NCT-02134925) (15). Twenty-seven percent (27%) of the vaccinated participants responded to the vaccine. In addition to the immune response, in this trial we evaluated adenoma recurrence by follow-up colonoscopy ≥ 1 year from the start of vaccination. In vaccine responders, adenoma recurrence was reduced by 38% compared to non-responders and placebo controls. Predictable factors such as gender, age, and HLA-type were not significantly different between vaccine responders and non-responders. It became important to understand why some individuals mounted a potentially protective immune response, while others did not, having the same diagnosis.

In this study, we analyzed PBMC samples collected from both trials at baseline (pre-vaccination) and 2 weeks post-first of 3 vaccines (week 0, week 2 and week 10) from vaccine responders and non-responders and identified comprehensive gene and pathway biomarkers related to vaccine response. We discovered that several key T- and B-cell cellular proliferation and stress pathways were enriched in responders, while oxidative phosphorylation and DNA damage response and repair pathways were enriched in non-responders. Responders had higher frequencies of CD4 cells at baseline, with higher activation and/or costimulatory signaling in CD8 and CD4 T-cells from baseline to week 2 in CD8 T-cells. Phosflow analysis revealed enhanced phosphorylation of B-cell signaling molecules and T-cell help targets in responders at baseline and a significant increase in NF κ B phosphorylation in B-cells at week 2. Lastly, we applied graphical modeling approaches (16–18) to this data and built a regression model to discriminate future responders and non-responders via their predicted and actual IgG response at week 12.

Materials and methods

Cohort and sample collection

PBMC samples from 69 individuals with a history of, or with newly diagnosed, advanced colonic adenoma and at high risk for colon cancer were collected for this study as part of two clinical trials of a MUC1 vaccine registered at clinicaltrials.gov (NCT-007773097, NCT-02134925) (14, 15). The vaccine, composed of 100 µg of MUC1 peptide plus the polyICLC adjuvant Hiltonol[®], was administered at week 0, 2, 10 and 52. The ethics committee/IRB of the following institutions gave ethical approval for this work: Mayo Clinic, Rochester MN; Kansas City Veterans Affairs Medical Center, Kansas City, KS; University of Pittsburgh Medical Center, Pittsburgh PA; University of Puerto Rico, San Juan PR; Thomas Jefferson University Hospital, Philadelphia PA; and Massachusetts General Hospital, Boston MA. All participants provided written informed consent. Blood samples were processed within 24 hours by the same individual, using the same protocol. Heparinized blood was layered on lymphocyte separation medium (MPbio) and centrifuged at 800 g for 10 min with lowest acceleration and deceleration speed. PBMC were collected from the interphase, washed twice, resuspended in 80% human serum and 20% DMSO, and stored in liquid nitrogen.

RNA-Seq

PBMC samples were thawed, pelleted, and lysed in 350 µL of RLT with beta-mercaptoethanol. RNA was isolated using the RNeasy Mini kit (Qiagen). RNA quality was assessed with the Fragment Analyzer (Agilent) and its Standard Sensitivity RNA kit. Total RNA was normalized to 100 ng prior to random hexamer priming and libraries generated by the TruSeq Stranded Total RNA – Globin kit (Illumina). The resulting libraries were assessed on the Fragment Analyzer (Agilent) with the High Sense Large Fragment kit and quantified using a Qubit 3.0 fluorometer (Life Technologies). Medium depth sequencing (>30 million reads per sample) was performed with a HiSeq 2500 (Illumina) on a high output, 125 base pair, paired end run.

Bioinformatic analysis

Raw demultiplexed fastq paired end read files were trimmed of adapters and filtered using the program skewer (19), discarding those with an average phred quality score <30 or a length <36. Trimmed reads were aligned to human reference genome GRCh38 using HISAT2 (20) and sorted using SAMtools (21). Aligned reads were counted and assigned to gene meta-features using the program featureCounts (22) as part of the Subread package. Quality control, normalization and analysis were performed in R, using an in-house pipeline utilizing the limma-trend method for differential gene expression testing and the GSEA (23) library for gene set sample enrichment. Biological sex and clinical trial batches were corrected for as blocking factors during modeling. Final differential gene expression

lists were filtered to remove non-coding RNAs as well as LOC features. The datasets for this study can be found in the Gene Expression Omnibus (GEO) public database with the accession number pending.

Flow cytometric analysis

For immune cell phenotyping and assessment of intracellular levels of bcl2, and phosphorylation of STAT3, erk1/2, NF-κB and MTORC targets, cells were first stained with Live/Dead Aqua (Invitrogen) followed by cocktails of monoclonal antibodies recognizing the following cell surface markers: CD4, CD8, CD45RA, CD27, CCR7, CD152, CD86, CD275, CD11c, CD56, CD16, CD19, CD3, HLA-DR, CD14, CD40, and CD11b. Cells were washed, fixed and permeabilized, then stained with antibodies specific for the following intracellular proteins: NFκB p65, erk1/2 (pT202/pY204), STAT3 (pY705), Akt1, pS6 (S235/236 & S240) and p4E-BP1 (T36/46). Cells were washed and fixed and events were collected on a BD ARIA-SORP instrument. A 15-minute incubation at 37C with recombinant human IL-6 (100ng/mL) (BD Pharmingen) was performed to induce NFκB signaling. After washing, cells were resuspended in staining buffer and sorted on an ARIA-SORP. Additional information on the panel of antibodies used for flow cytometric analysis can be found in [Supplementary Table 1](#). Data was analyzed using FlowJo software (TreeStar).

Predictive model for post-vaccination immune response

A detailed explanation of computational model development and evaluation can be found in the [Supplementary Materials](#). Briefly, a LASSO logistic regression (24) was used to develop a prediction model for a binary outcome of response defined by the clinical trial endpoint (≥ 2 -fold increase in IgG from baseline to week 12), using transcriptomic data measured two-weeks post-vaccination (Week 2 data). A Mixed Graphical Models (MGM) algorithm was used to infer a unidirectional graphical model followed by FCI-MAX to determine direction. All statistical analysis was performed in R.

Statistics

Unless otherwise indicated, the Student's t-test was used with $p \leq 0.05$ chosen as the level of significance. Adjusted p-values are shown in [Figures 1–5](#) at $p \leq 0.2$ and $p \leq 0.1$ levels but were not used in tests for significance.

Results

Vaccine responders and non-responders show differential gene expression in PBMCs pre-vaccination

Next-generation RNA-seq analysis was performed on PBMCs from vaccinees. We assayed PBMC samples collected prior to the

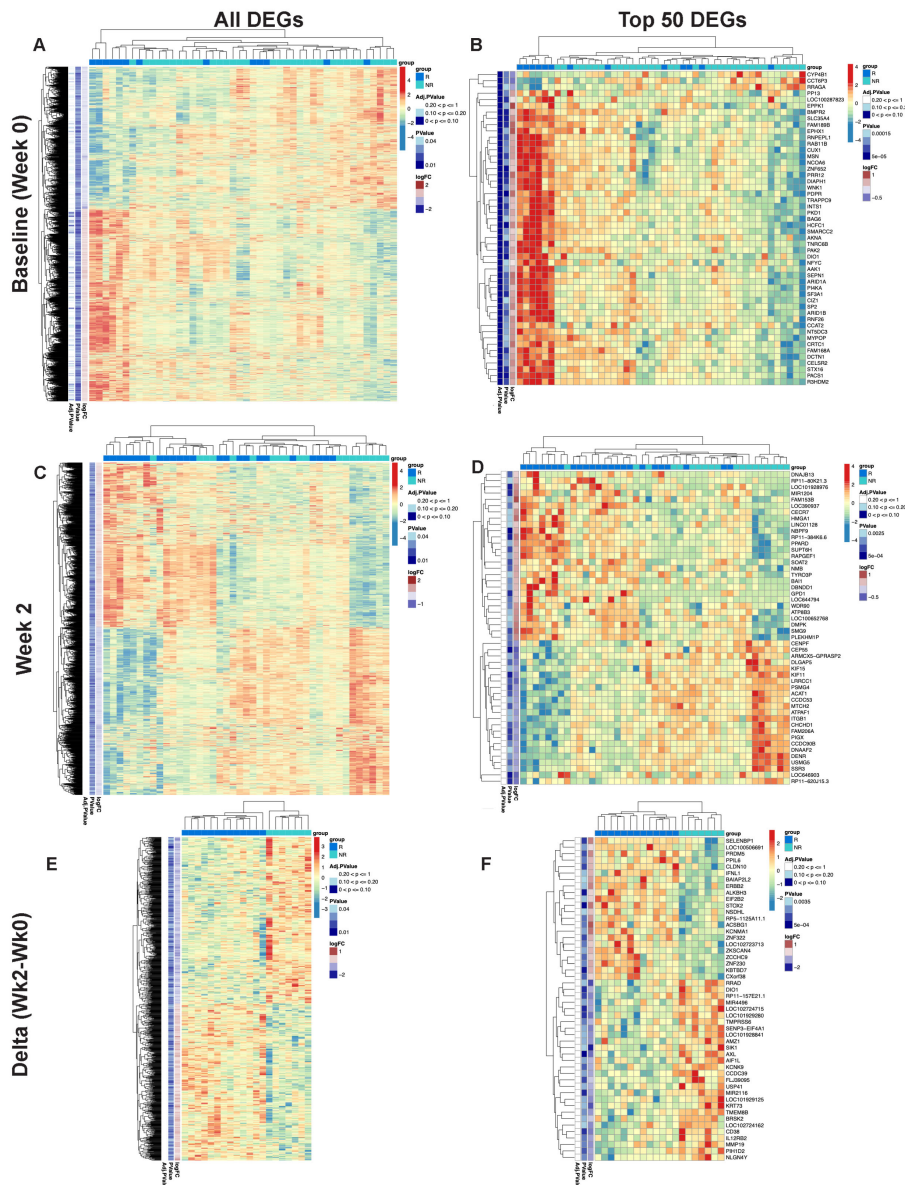


FIGURE 1
 Differential gene expression pre- and post-MUC1 vaccination in responders and non-responders. All differentially expressed genes (DEGs) are shown in two-way hierarchical heatmaps for each time point and contrast in the left column and top 50 DEGs by p-value are shown in the right column. Group status is indicated in the row above the heatmap with responders (R) in dark blue, and non-responders (NR) in light blue. Z-scored normalized gene expression for each gene is displayed horizontally across all samples (diverging color scale legend on the upper right of each heatmap). Log2 fold-change, p-values (all $p \leq 0.05$) and adjusted p-values are indicated in labelled vertical columns. Hierarchical clustering of the samples is indicated by the dendrogram at the top of heatmap, while clustering of the genes is indicated at the far left. Heatmaps showing all DEGs pre-vaccination (Baseline/Week 0) (A) top 50 DEGs pre-vaccination (Baseline/Week 0) (B), DEGs at Week 2 post-vaccination (C), top 50 DEGs at Week 2 post-vaccination (D), all genes demonstrating longitudinal changes at Week 2 vs. Week 0 (Delta Wk2-Wk0) (E), top 50 genes demonstrating longitudinal changes at Week 2 vs. Week 0 (Delta Wk2-Wk0) (F) in PBMCs from responders versus non-responders. Available samples from responders and non-responders for analysis were $n=13$ and 33 , respectively, in (A, B), $n=24$ and 19 , respectively, in (C, D), and $n=13$ and 7 , respectively, for the paired analysis in (E, F).

first injection (baseline) and 2 weeks later, at the time of the second injection to be able to define preexisting (at baseline) and early post-vaccination (week 2) signatures of later response to MUC1 vaccination. Vaccine responders (R, $n=24$) in both trials were defined as having anti-MUC1 IgG levels at week 12 (after all three injections) at least two-fold higher than baseline, while non-responders (NR, $n=45$) showed no difference from baseline. Responder and non-responder donor numbers varied at each

time point due to sample collection limitations within the clinical trials. For some of our analyses we also classified responders by antibody levels into high responders (HR, anti-MUC1 IgG OD450 at 1:80 plasma dilution ≥ 0.4) and low responders (LR, OD450 at 1:80 plasma dilution < 0.4).

RNA-seq performed on PBMCs collected immediately pre-vaccination (baseline) revealed a total of 2,321 genes that were differentially expressed between all responders and all non-

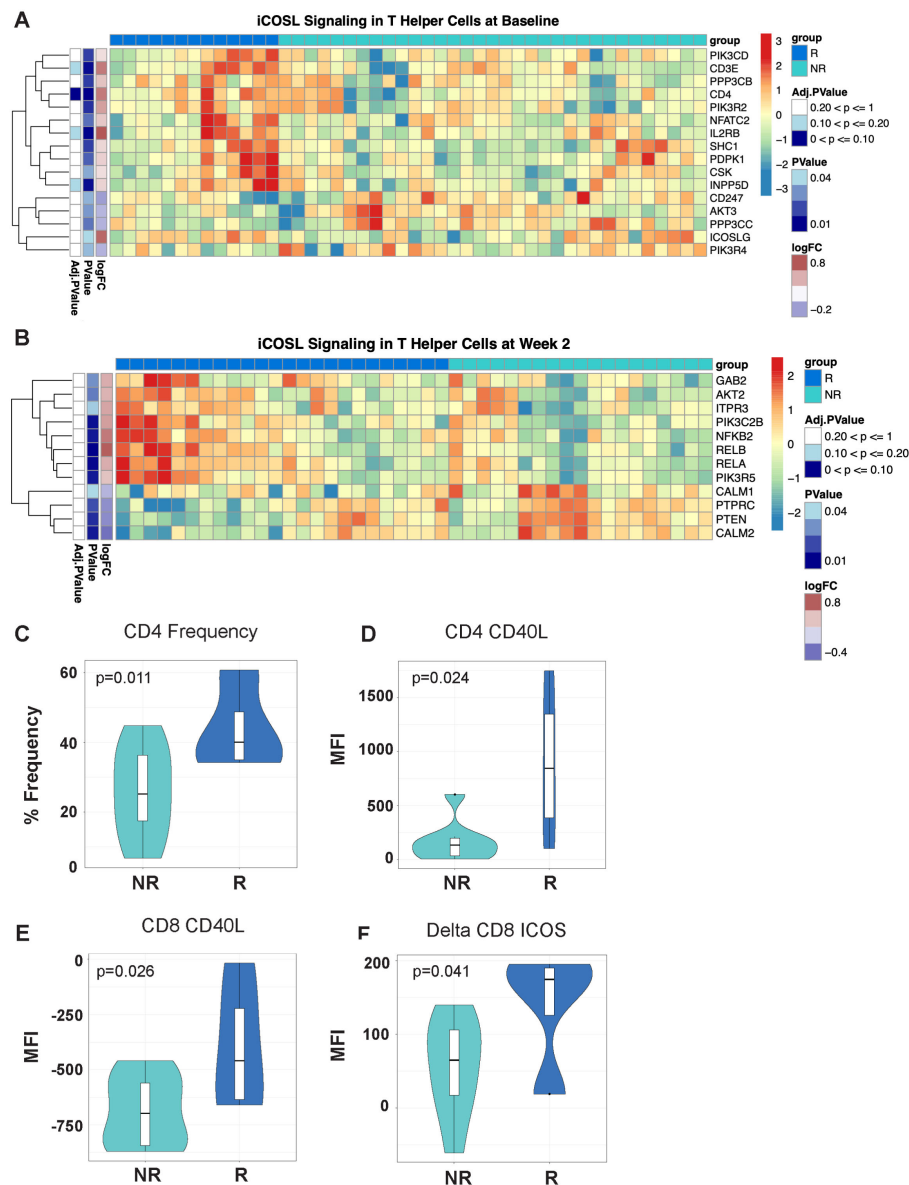
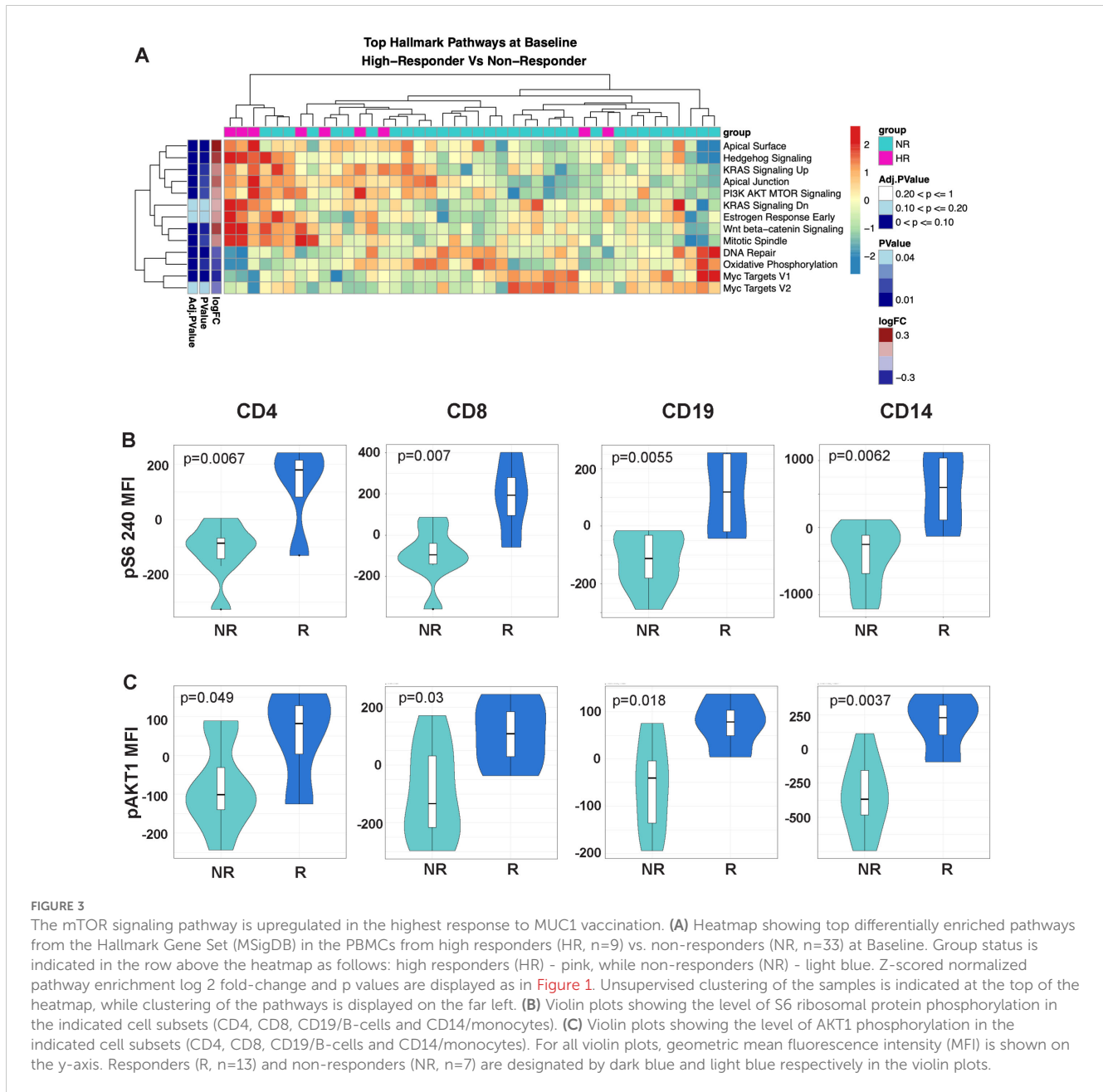


FIGURE 2

Differentially expressed T-cell fitness signatures in PBMCs from responders and non-responders to MUC1 vaccination is associated with CD4 frequencies and expression of multiple regulators of T-cell help. (A, B) iCOSL signaling pathway-related genes are associated with response to MUC1 vaccination at Baseline (A) and Week 2 post-vaccination (B) in MUC1 vaccine responders and non-responders. Heatmaps are organized as in Figure 1. Violin plots of CD4+ T-cell frequencies as determined by flow cytometry. (C) Violin plots of CD40L expression on CD4 T-cells (D), CD8 T-cells (E), and the change in ICOS levels on CD8 T-cells (Delta Week 2 vs. Week 0/Baseline) (F) measured by geometric mean fluorescence intensity (MFI). Samples from responders and non-responders were n=13 and 33, respectively, in (A), n=24 and 19, respectively, in (B), and n=13 and 7, respectively, in (C-F).

responders at baseline (see two-way hierarchical clustering overview in Figure 1A). Within these genes, 1,337 showed increased transcript levels and 984 showed decreased levels. Among the top 50 differentially expressed genes by p-value (Figure 1B), 47 genes were upregulated in responder relative to non-responder subgroups. The upregulated genes were involved in transcriptional and epigenetic regulation, including multiple subunits of the SWI/SNF chromatin remodeling complex (ARID1A, ARID1B, and SMARCC2), as well as NCOA6, a

multifunctional transcriptional coactivator and component of the Set1-like H3K4-methyltransferase complex ASCOM, all of which have been shown to play a role in the pathogenesis of cancer (25). Additional cancer-relevant transcriptional regulators higher in responders before vaccination include SP2, NFYC, AKNA, MYPOP, and ZNF652. CUX1 is a subunit of the NF- μ NR repressor that binds to the matrix attachment regions of the immunoglobulin heavy chain enhancer and the TCR enhancer. The epigenetic regulator HCFC1 tethers Set and Sin3 histone



modifying complexes together and was also higher in responders at baseline (26). We observed an increase in TRAPPC9, an activator of NF κ B, and FAM168A, which is involved in the PI3K/AKT/NF κ B signaling pathway. RRAGA was one of 3 downregulated genes among the top differentially expressed genes in responders and plays a role in regulating the mTORC1 complex (27). The presence of transcriptional and epigenetic regulators within the list of upregulated genes could explain the large number of significant changes in steady-state RNA levels we observed and suggests a differing global transcriptional program between responders and non-responders before vaccination. As these upstream regulators have the potential to broadly remodel the transcriptome, they may represent potent therapeutic targets.

Vaccine responders and non-responders show differences in gene expression in PBMCs at week 2 post-vaccination

At two weeks post-first injection, we found 1,887 genes differentially expressed in responders vs. non-responders, 934 genes upregulated and 953 genes downregulated (see two-way hierarchical clustering overview in Figure 1C). The top 50 genes arranged by p-value are shown in Figure 1D. Among the upregulated genes are several cancer-related transcriptional regulators including PPAR δ (28) and HMGA1 (29), key regulators of lipid pathways (30), transcription elongation factor SPT6 (SUPT6H), SOAT2, an enzyme involved in lipoprotein and cholesterol regulation, and GPD1, an enzyme that

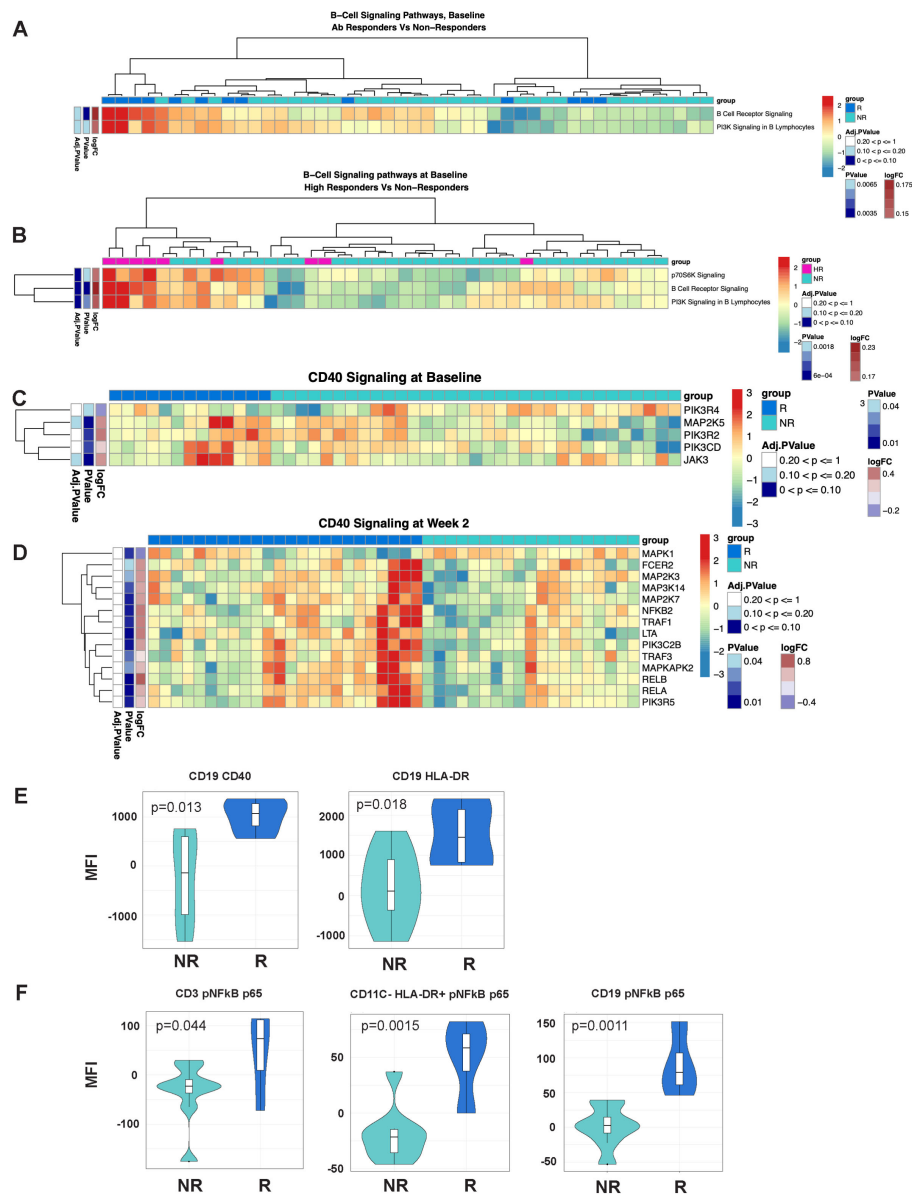


FIGURE 4

B-cell signaling and NFκB signaling signatures are associated with response to MUC1 vaccination. (A, B) Heatmaps showing enrichment of B-Cell Receptor Signaling pathways in the PBMCs from Responders (R) vs. non-responders (NR) at Baseline (A) and high responders (HR, n=9) vs. non-responders (NR) at Baseline (B). (C, D) Differential gene expression from the CD40 Signaling pathway from PBMCs from R vs. NR at Baseline (C) and Week 2 (D). Heat maps are organized as in Figure 1. (E) Violin plots showing expression levels of CD40 and HLA-DR on B-cells (CD19+). (F) Violin plots of NFκB complex p65 subunit phosphorylation in T-cells (CD3+), non-DC/non-B antigen presenting cells (CD11C-HLADR+), and B-cells (CD19+). For violin plots, geometric mean fluorescence intensity (MFI) is shown on the y-axis. Samples from responders and non-responders were n=13 and 33, respectively, in (A, C), n=24 and 19, respectively, in (D). Responders (R, n=13) and non-responders (NR, n=7) are designated by dark blue and light blue respectively in the violin plots.

plays a key role in lipid metabolism, are also upregulated in responders. Among the downregulated cancer-related genes we found five involved in mitosis and G2/M DNA replication checkpoint, the kinesin-like proteins KIF11 and KIF15 (31), centromere/centrosome proteins CENPF and CEP55 (32), and the cell cycle regulator protein DLGAP5 (33). Importantly, CEP55 and DLGAP5 are key predictors of antibody response in our graphical model discussed below.

We then performed double contrast analysis to identify genes that were significantly differentially changed from baseline

in paired samples from the same responders and non-responders at 2 weeks (Figure 1E). The top 50 genes by p-value (Figure 1F) are enriched in immune-related genes. IFNL1 is upregulated in contrast to CD38 and IL12RB2, which are downregulated in responders. Again, selective upregulation of transcriptional and epigenetic regulators in responders is evident; examples include PRDM5, ZNF230, ZCCHC9, ZKSCAN4, and the epigenetic regulator ALKBH3, which demethylates DNA and RNA in cancer cells (34).

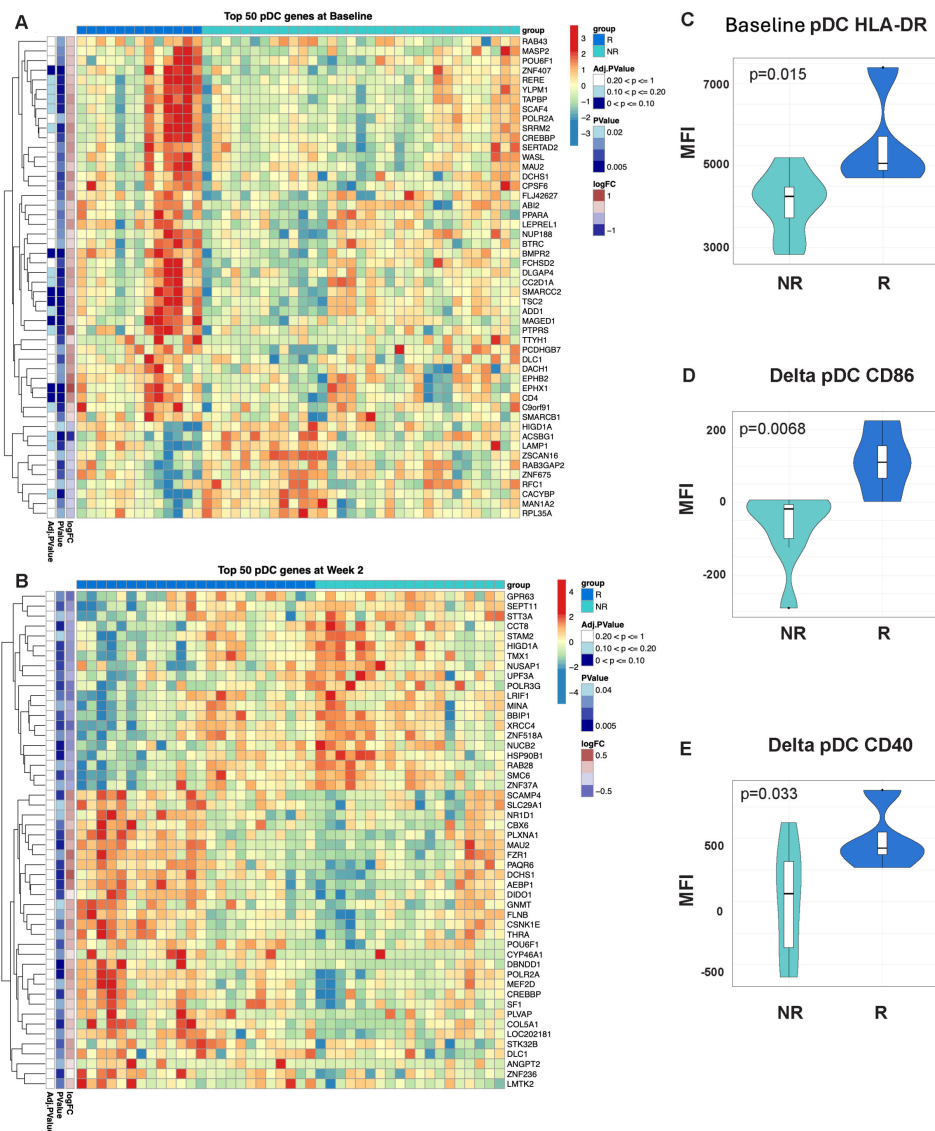


FIGURE 5

Signatures of enhanced antigen presentation are evident in participants with an enhanced response to MUC1 vaccination. Heatmaps showing enrichment of dendritic cell (DC) specific genes in the PBMCs from Responders (R) vs. non-responders (NR) at Baseline (A) and Week 2 post-vaccination (B). Heatmaps are organized as in Figure 1. Violin plots of HLA-DR expression on DCs at Baseline (Week 0) (C), as well relative change in expression of CD86 (D) and CD40 (E) in these cells. For all violin plots, geometric mean fluorescence intensity (MFI) is shown on the y-axis. Samples from responders and non-responders were $n=13$ and 33 , respectively, in (A), $n=24$ and 19 , respectively, in (B). Week 2 vs. baseline paired responders (R, $n=13$) and non-responders (NR, $n=7$) are designated by dark blue and light blue respectively in the violin plots.

ICOS/ICOSL signaling is differentially associated with response to the MUC1 vaccine

We performed gene set variation analysis (GSVA) on baseline gene expression data to identify biological pathways regulating the response to vaccination. Vaccine responders displayed significant upregulation of genes involved in the ICOS-ICOSL pathway in T-helper Cells signaling pathway, with increased expression of multiple genes both at baseline and week 2 post-vaccination (Figures 2A, B, respectively). At baseline, responders expressed higher levels of ICOSL, IL2RB, and CD4 coreceptor genes, while at week 2 post-vaccination higher levels of the

downstream NFKB pathway genes including NFKB2, RELB and RELA were evident.

By flow cytometry, we detected significant differences in the expression of key proteins involved in ICOS/ICOSL signaling. We determined that higher frequencies of CD4 T-cells were present in responders at baseline (Figure 2C). Notably, CD4 and CD8 T-cells in responders had higher levels of CD40L expression prior to vaccination (Figures 2D, E respectively). Greater increases in ICOS expression were detected post-vaccination in CD8 T-cells of responders (Figure 2F). The baseline immune signature in responders, characterized by T cells with increased CD40L expression, may enhance ICOS/ICOSL signaling by promoting strong interactions with antigen presenting cells (APCs) and facilitate T cell activation and function.

mTOR signaling is upregulated in responders to MUC1 vaccination

As many components of the ICOS/ICOSL pathway were significantly higher in the responders vs. non-responders, we focused on differences in the mTOR signaling pathway which lies directly downstream of ICOS/ICOSL engagement. Top enriched pathways in high responders vs. non-responder comparisons included PI3K/AKT/MTOR signaling, WNT/beta-catenin signaling and hedgehog signaling (Figure 3A). In contrast, the Myc targets V1 pathway and DNA repair were negatively associated in high responders.

To validate enhanced mTOR signaling in responders, we measured the phosphorylation levels of RPS6, a commonly used readout of mTORC1 activity, by phosflow. There was a greater increase in RPS6 phosphorylation in CD4 and CD8 T-cells, B-cells (CD19), and monocytes (CD14) of responders, an observation validating our finding at the phosphoprotein level (Figure 3B). We also performed intracellular staining targeting the phosphorylated AKT1 kinase upstream of the MTORC1 signaling complex. Similarly, we found a greater increase in AKT1 phosphorylation in responders compared to non-responders.

B-cell signaling and enhanced antigen presentation signatures are positively associated with response to MUC1 vaccination

As ICOS/ICOSL-mediated signaling promotes fitness of the T lymphocyte compartment, we hypothesized that signaling from the T-cells to the B-cell and APC compartment was also differentially induced. Pathway enrichment analysis of the transcriptomic data revealed significant enrichment of B-Cell Receptor Signaling and PI3K Signaling in B Lymphocytes pathways at baseline (Figures 4A, B) and NFκB and CD40 Signaling pathways at baseline and at week 2 post-vaccination (Figures 4C, D). CD40 receptor engagement on the surface of antigen presenting cells, such as B-cells, leads to activation of NFκB signaling and enhanced cellular survival and function. Notably, multiple signaling component genes (MAP kinases and Jak3) are significantly upregulated in responders at baseline, followed by upregulation of additional signaling molecules at week two (TRAF1, TRAF3, NFKB1, NFKB2, RELA and RELB).

We validated increased expression of CD40 and HLA-DR on B-cells (CD19+) in responders (Figure 4E) using flow cytometric analyses. We used an intracellular phosflow panel to detect phosphorylation of the p65 subunit of NFκB. We found increased IL6-induced NFκB signaling via phosphorylation of p65 in T-cells, HLA-DR+ non-B/non-DC APCs and B-cells of responders (Figure 4F), and B-cells of high responders expressing significantly higher levels of HLADR compared to non-responders (Figure 4E).

Finally, we performed gene set variation analysis using a published collection of gene sets associated with immunogenicity to influenza vaccination (35). We determined that a plasmacytoid

dendritic cell (DC) signature was already enriched in the PBMCs of responders at baseline (Figure 5A) and further enriched at week 2 post-vaccination (Figure 5B). Vaccine responders showed increased HLA-DR levels on DCs (CD3-, CD19-, HLA-DR+, CD11c+) at baseline (Figure 5C). Responders also showed a greater relative change in CD86 and CD40 expression from baseline to two weeks (Figures 5D, E). Altogether, these results indicate that additional signatures of enhanced antigen presentation are associated with enhanced response to MUC1 vaccination.

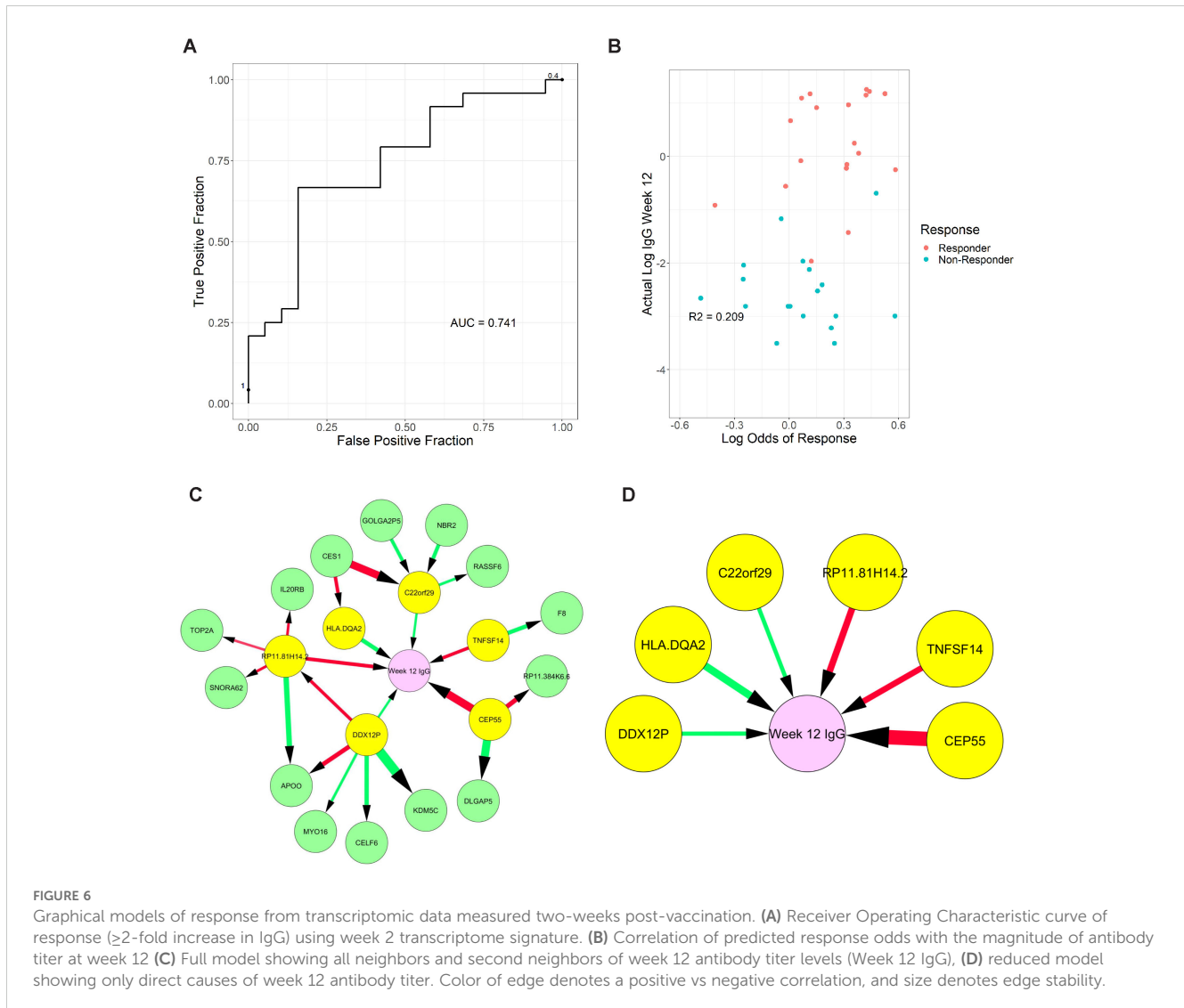
Six differentially expressed transcripts 2 weeks post-vaccination predict week 12 IgG response to the MUC1 vaccine

Based on evidence of key differences in cell populations and molecular pathways between responders and non-responders at baseline and post-vaccination, we hypothesized that some differentially expressed genes may be useful for patient selection and outcome prediction. We tested this hypothesis by applying LASSO regression and MGM-FCI-MAX (18), a graphical modeling algorithm, to 7,968 transcripts meeting a minimal variance threshold. We first performed a cross-validation experiment (see Supplementary Materials) to assess the ability to predict antibody response to the vaccine at week 12, using the transcriptomic signatures at week 2 post-vaccination. Our model achieved an area under the receiver operating characteristic curve (AUROC) value of 0.741 to predict response vs. non-response (Figure 6A). At a predicted probability threshold of 0.5, the model achieved a sensitivity of 91.7% (22 predicted responders/24 true responders) and a specificity of 36.8% (7 predicted non-responders/19 true non-responders). Predicted response odds were correlated with the magnitude of antibody titer at week 12 ($R^2 = 0.209$, $p < 0.001$) (Figure 6B), and with the ratio of IgG titer at week 12 versus baseline ($R^2 = 0.147$, $p = 0.015$).

Next, we used graphical models to determine the variables directly linked to week 12 antibody titer and distinguish them from simple correlates. We produced a full model with all genes selected in the previous cross-validation experiments, which were learned using the entire week 2 dataset (Figure 6C). Finally, we identified 6 genes that are directly linked to week 12 antibody titer: RP11.81H14.2, CEP55, and TNFSF14 (negatively associated) and C22orf29, DDX12P, and HLA-DQA2 (positively associated) (Figure 6D). The role of these transcripts and how they may contribute to the induction of immune response and vaccine efficacy (discussed below) warrants further investigation.

Discussion

Therapeutic cancer vaccines, tested in numerous clinical trials over several decades, failed to realize the promise generated by the discovery of tumor antigens capable of eliciting humoral and cellular immunity. In most cases, vaccines administered after primary tumor removal failed to boost anti-tumor immunity and prevent tumor recurrence. Ultimately, a greater understanding of the many



immunosuppressive forces in the tumor microenvironment helped to explain the reduced efficacy of therapeutic vaccines. These discoveries support preventative vaccines as an alternative approach to cancer vaccination to reduce cancer risk and incidence as they could be applied in the absence of cancer and cancer-induced immunosuppression. The two clinical trials from which we derived the PBMCs, applied this preventative approach by vaccinating individuals without cancer but at high risk for colon cancer due to advanced colonic adenoma diagnosis (14, 15). We expected a vaccine response from most individuals, measured by the production of anti-MUC1 IgG antibodies. Anti-MUC1 IgG was selected as a convenient as well as appropriate biomarker of the vaccine immunogenicity and potential efficacy. The switch from IgM to IgG requires MUC1 specific T cell help, indicating that both the B cell and the T cell compartments were activated by the vaccine. Furthermore, as MUC1 is a cell surface tumor antigen, MUC1 antibodies can target tumor cells for destruction by antibody-mediated cellular cytotoxicity (ADCC) and antibody-mediated phagocytosis (ADCP). It came as a surprise that only a subset of participants produced high levels of anti-MUC1 antibodies in response to the vaccine and established a

long-lasting memory response. These results indicate that the vaccine was capable of inducing immunity and the response was determined by the individuals receiving the vaccine. Mechanisms underlying this variable response to an apparently efficacious vaccine were not clear.

To address this major knowledge gap with an unbiased approach, we performed RNA-seq on total PBMCs from participants in the two MUC1 peptide vaccine trials to identify genes and pathways differentially regulated at baseline as well as post-vaccination in the participants that responded versus those that failed to respond to the vaccine. The analysis revealed that vaccine responders at baseline exhibited an enrichment of key pathways governing survival and proliferation in immune cells, such as mTOR and NF κ B signaling, as well as increased frequencies of CD4 and CD8 T-cells. There were more memory CD8 T-cells at baseline and week 2 (post MUC1 vaccine) in responders (Figures 2A, E). Responders also had more CD4 T-cells at baseline and higher frequencies of memory CD4 T-cells at week 2 (Figures 2A, C, D). Other immune compartments appeared to differ in favor of responders with higher levels of BCL2 expression at baseline in CD14+ and greater increases in BCL2 expression at week

2 post-vaccination (data not shown). The control of DC longevity by the regulation of BCL2 directly impacts immune responses. Higher levels of BCL2 suggest enhanced survival in the myeloid compartment and consequently better antigen presentation.

The differentially expressed genes and pathways that we have identified in vaccine responders and non-responders pre-vaccination and two weeks post-vaccination are top candidates for early biomarkers of vaccine immunogenicity at week 12. Among the six genes directly linked to MUC1 antibody production at week 12, some have already been identified as diagnostic biomarkers (CEP55, TNFSF14) while the others merit deeper investigation as they hold the potential to enhance our understanding of vaccine response. Overexpression of CEP55 has been observed in numerous cancer cell types, including premalignant lesions of the colon (36), and is a known correlate of poor prognosis (37). Notably, a CEP55 peptide vaccine was proposed for breast and colorectal carcinoma immunotherapy as CEP55 is involved in the PI3K/Akt signaling pathway. TNFSF14, also known as LIGHT, functions as a co-stimulatory factor for the activation of lymphoid cells and modulates T-cell proliferation (38, 39). HLA-DQA2 codes for the alpha chain of the HLA-DQ complex and is primarily involved in antigen presentation (38). Interestingly, HLA-DQ phenotypes have been linked with non-responsiveness to hepatitis B vaccination (40). DDX12P is an m⁶A-associated prognostic pseudogene, correlated with favorable outcomes in patients with head and neck squamous cell carcinoma (41). Furthermore, expression patterns of DDX12P were correlated with anti-tumor response and may regulate immune-involved genes through miRNA targeting. RP11-81H14.2 (LINC02384) is a long intergenic non-coding RNA primarily expressed in TH1 cells (42). Little is known about the function of LINC02384; however, it has been proposed to act as a competitive endogenous RNA of IL2RA and IL7R by reducing available shared regulatory miRNAs (43). C22orf29 (also known as RTL10) may have the capacity to induce apoptosis in a BH3 domain-dependent manner, presumably by engaging the Bcl2 family regulatory network to modulate the intrinsic apoptotic signaling pathway (44). The identification of known diagnostic biomarkers and immunotherapy targets within our predictive genes lends credence to the graphical models utilized in this study.

Given the cancer immunoprevention potential of the MUC1 peptide vaccine response, characterized by a reduction of adenoma recurrence (15), the differentially expressed genes and regulated pathways we identified hold promise as therapeutic targets for vaccine non-responders. While these observations were made on responders and non-responders to the MUC1 vaccine, it is likely that a number of these differentially enriched genes and pathways play a role in other vaccine responses. Many vaccines do not elicit a response in all recipients, such as the yearly flu vaccine which varies in effectiveness between 40% and 60% (45). The selected adjuvant for the MUC1 vaccine, polyICLC, excels at activating dendritic cells to promote type I (innate) immunity (46). Alternative adjuvants may need to be considered for non-responders to the MUC1 peptide adjuvanted with polyICLC. While efforts are often made to improve the vaccine, it also may be important to consider an individual's incoming immune history to respond to the vaccine. Indeed, numerous research studies have demonstrated a correlation between the immune status prior to vaccination and the subsequent antibody

response (47–49). Overall, individuals that responded to the MUC1 vaccine showed a greater readiness in all the immune compartments to present and respond to antigen. The ability to profile individuals as potential responders or non-responders can aid in the selection of those who benefit most from a particular vaccine. At the same time, understanding the barriers to response in non-responders can inform the development of better vaccine designs suitable for specific immune genotypes and phenotypes.

Data availability statement

The data presented in the study are deposited in the NCBI Gene Expression Omnibus repository, accession number GSE278476.

Ethics statement

The studies involving humans were approved by the Institutional Review Boards of Mayo Clinic, Rochester MN; Kansas City Veterans Affairs Medical Center, Kansas City, KS; University of Pittsburgh Medical Center, Pittsburgh PA; University of Puerto Rico, San Juan PR; Thomas Jefferson University Hospital, Philadelphia PA; and Massachusetts General Hospital, Boston MA. The studies were conducted in accordance with the local legislation and institutional requirements. The participants provided their written informed consent to participate in this study.

Author contributions

CC: Conceptualization, Formal Analysis, Methodology, Validation, Writing – original draft, Writing – review & editing. VR: Formal Analysis, Methodology, Writing – original draft. BR: Data curation, Formal Analysis, Methodology, Writing – original draft. LZ: Validation, Writing – original draft. BT: Methodology, Writing – original draft. JG: Formal Analysis, Methodology, Writing – original draft. MC: Methodology, Writing – original draft. RS: Investigation, Writing – review & editing, Funding acquisition. OF: Conceptualization, Formal Analysis, Funding acquisition, Investigation, Methodology, Validation, Writing – original draft, Writing – review & editing. PB: Conceptualization, Formal Analysis, Funding acquisition, Investigation, Methodology, Validation, Writing – original draft, Writing – review & editing. MC: Conceptualization, Formal Analysis, Funding acquisition, Investigation, Methodology, Validation, Writing – original draft, Writing – review & editing.

Funding

The author(s) declare that financial support was received for the research, authorship, and/or publication of this article. This research was supported by NCI and NHLBI funding to OF (R35CA210039), PB (R01HL159805), and MC (P30CA043703 Sub-Project 9867). VR was supported by a fellowship through the T32CA082084 grant.

Acknowledgments

We appreciate the tremendous efforts of the team members that conducted the two clinical trials and provided samples for this study, particularly Lisa Boardman, Marcia Cruz-Correa, Ajay Bansal, David Kastenber, Chin Hur, Lynda Dzubinski, Sharon Kaufman, Luz M Rodriguez, Ellen Richmond, Asad Umar, Eva Szabo, Andres Salazar, John McKolanis, Pamela Beatty, Reetesh Pai, Aatur Singhi, Camille Jacqueline, Riyue Bao, Brenda Diergaarde, Ryan McMurray, Carrie Strand, Nathan Foster, David Zahrieh, and Paul Limburg. We are also indebted to all the trial participants for their commitment to our cancer prevention mission. We thank the Genomics Core at the Lerner Research Institute of Cleveland Clinic and the Genomics and Applied Functional Genomics Cores at Case Western Reserve University for their technical and analytical support.

Conflict of interest

Author RS reports support from Freenome, Exact Sciences, and Immunovia during the conduct of the study. Author OF reports personal fees from PDS Biotech, Invectys, Immodulon, and Ardigen outside the submitted work.

References

- Zitvogel L, Perreault C, Finn OJ, Kroemer G. Beneficial autoimmunity improves cancer prognosis. *Nat Rev Clin Oncol.* (2021) 18:591–602. doi: 10.1038/s41571-021-00508-x
- Jacqueline C, Finn OJ. Antibodies specific for disease-associated antigens (DAA) expressed in non-malignant diseases reveal potential new tumor-associated antigens (TAA) for immunotherapy or immunoprevention. *Semin Immunol.* (2020) 47:101394. doi: 10.1016/j.smim.2020.101394
- Finn OJ, Rammensee HG. Is it possible to develop cancer vaccines to neoantigens, what are the major challenges, and how can these be overcome? Neoantigens: nothing new in spite of the name. *Cold Spring Harb Perspect Biol.* (2018) 10. doi: 10.1101/cshperspect.a028829
- Gnjatic S, Bronte V, Brunet LR, Butler MO, Disis ML, Galon J, et al. Identifying baseline immune-related biomarkers to predict clinical outcome of immunotherapy. *J Immunother Cancer.* (2017) 5:44. doi: 10.1186/s40425-017-0243-4
- Liu J, Fu M, Wang M, Wan D, Wei Y, Wei X. Cancer vaccines as promising immuno-therapeutics: platforms and current progress. *J Hematol Oncol.* (2022) 15:28. doi: 10.1186/s13045-022-01247-x
- Gordon B, Gadi VK. The role of the tumor microenvironment in developing successful therapeutic and secondary prophylactic breast cancer vaccines. *Vaccines (Basel).* (2020) 8. doi: 10.3390/vaccines8030529
- Tie Y, Tang F, Wei YQ, Wei XW. Immunosuppressive cells in cancer: mechanisms and potential therapeutic targets. *J Hematol Oncol.* (2022) 15:61. doi: 10.1186/s13045-022-01282-8
- Kimura T, McKolanis JR, Dzubinski LA, Islam K, Potter DM, Salazar AM, et al. MUC1 vaccine for individuals with advanced adenoma of the colon: a cancer immunoprevention feasibility study. *Cancer Prev Res (Phila).* (2013) 6:18–26. doi: 10.1158/1940-6207.CAPR-12-0275
- Ramanathan RK, Lee KM, McKolanis J, Hitbold E, Schraut W, Moser AJ, et al. Phase I study of a MUC1 vaccine composed of different doses of MUC1 peptide with SB-AS2 adjuvant in resected and locally advanced pancreatic cancer. *Cancer Immunol Immunother.* (2005) 54:254–64. doi: 10.1007/s00262-004-0581-1
- Pantuck AJ, van Ophoven A, Gitlitz BJ, Tso CL, Acres B, Squiban P, et al. Phase I trial of antigen-specific gene therapy using a recombinant vaccinia virus encoding MUC-1 and IL-2 in MUC-1-positive patients with advanced prostate cancer. *J Immunother.* (2004) 27:240–53. doi: 10.1097/00002371-200405000-00009
- Bartsch R, Singer CF, Pfeiler G, Hubalek M, Stoeger H, Pichler A, et al. Conventional versus reverse sequence of neoadjuvant epirubicin/cyclophosphamide

The remaining authors declare that the research was conducted in the absence of any commercial or financial relationships that could be construed as a potential conflict of interest.

The author(s) declared that they were an editorial board member of Frontiers, at the time of submission. This had no impact on the peer review process and the final decision.

Publisher's note

All claims expressed in this article are solely those of the authors and do not necessarily represent those of their affiliated organizations, or those of the publisher, the editors and the reviewers. Any product that may be evaluated in this article, or claim that may be made by its manufacturer, is not guaranteed or endorsed by the publisher.

Supplementary material

The Supplementary Material for this article can be found online at: <https://www.frontiersin.org/articles/10.3389/fimmu.2024.1437391/full#supplementary-material>

SUPPLEMENTARY TABLE 1

Detailed information on antibody panels used for flow cytometric analysis.

- and docetaxel: sequencing results from ABCSG-34. *Br J Cancer.* (2021) 124:1795–802. doi: 10.1038/s41416-021-01284-2
- Schimanski CC, Kasper S, Hegewisch-Becker S, Schroder J, Overkamp F, Kullmann F, et al. Adjuvant MUC vaccination with tecemotide after resection of colorectal liver metastases: a randomized, double-blind, placebo-controlled, multicenter AIO phase II trial (LICC). *Oncoimmunology.* (2020) 9:1806680. doi: 10.1080/2162402X.2020.1806680
 - Ma P, Beatty PL, McKolanis J, Brand R, Schoen RE, Finn OJ. Circulating myeloid derived suppressor cells (MDSC) that accumulate in premalignancy share phenotypic and functional characteristics with MDSC in cancer. *Front Immunol.* (2019) 10:1401. doi: 10.3389/fimmu.2019.01401
 - Lohmueller JJ, Sato S, Popova L, Chu IM, Tucker MA, Barberena R, et al. Antibodies elicited by the first non-viral prophylactic cancer vaccine show tumor-specificity and immunotherapeutic potential. *Sci Rep.* (2016) 6:31740. doi: 10.1038/srep31740
 - Schoen RE, Boardman LA, Cruz-Correa M, Bansal A, Kastenber D, Hur C, et al. Randomized, double-blind, placebo-controlled trial of MUC1 peptide vaccine for prevention of recurrent colorectal adenoma. *Clin Cancer Res.* (2023) 29:1678–88. doi: 10.1158/1078-0432.CCR-22-3168
 - Sedgewick AJ, Buschur K, Shi I, Ramsey JD, Raghu VK, Manatakis DV, et al. Mixed graphical models for integrative causal analysis with application to chronic lung disease diagnosis and prognosis. *Bioinformatics.* (2019) 35:1204–12. doi: 10.1093/bioinformatics/bty769
 - Sedgewick AJ, Shi I, Donovan RM, Benos PV. Learning mixed graphical models with separate sparsity parameters and stability-based model selection. *BMC Bioinf.* (2016) 17 Suppl 5:175. doi: 10.1186/s12859-016-1039-0
 - Raghu VK, Ramsey JD, Morris A, Manatakis DV, Sprites P, Chrysanthis PK, et al. Comparison of strategies for scalable discovery of latent variable models from mixed data. *Int J Data Sci Anal.* (2018) 6:33–45. doi: 10.1007/s41060-018-0104-3
 - Jiang H, Lei R, Ding SW, Zhu S. Skewer: a fast and accurate adapter trimmer for next-generation sequencing paired-end reads. *BMC Bioinf.* (2014) 15:182. doi: 10.1186/1471-2105-15-182
 - Kim D, Langmead B, Salzberg SL. HISAT: a fast spliced aligner with low memory requirements. *Nat Methods.* (2015) 12:357–60. doi: 10.1038/nmeth.3317
 - Yang J, Ding X, Sun X, Tsang SY, Xue H. SAMSVM: A tool for misalignment filtration of SAM-format sequences with support vector machine. *J Bioinform Comput Biol.* (2015) 13:1550025. doi: 10.1142/S0219720015500250

22. Liao Y, Smyth GK, Shi W. featureCounts: an efficient general purpose program for assigning sequence reads to genomic features. *Bioinformatics*. (2014) 30:923–30. doi: 10.1093/bioinformatics/btt656
23. Hanzelmann S, Castelo R, Guinney J. GSEA: gene set variation analysis for microarray and RNA-seq data. *BMC Bioinf*. (2013) 14:7. doi: 10.1186/1471-2105-14-7
24. Tibshirani R. Regression shrinkage and selection via the lasso. *J R Stat Society: Ser B (Methodological)*. (1996) 58:267–88. doi: 10.1111/j.2517-6161.1996.tb02080.x
25. Wang XX, Fu L, Li X, Wu X, Zhu Z, Fu L, et al. Somatic mutations of the mixed-lineage leukemia 3 (MLL3) gene in primary breast cancers. *Pathol Oncol Res*. (2011) 17:429–33. doi: 10.1007/s12253-010-9316-0
26. Wysocka J, Myers MP, Laherty CD, Eisenman RN, Herr W. Human Sin3 deacetylase and trithorax-related Set1/Ash2 histone H3-K4 methyltransferase are tethered together selectively by the cell-proliferation factor HCF-1. *Genes Dev*. (2003) 17:896–911. doi: 10.1101/gad.252103
27. Shen K, Valenstein ML, Gu X, Sabatini DM. Arg-78 of Nprl2 catalyzes GATOR1-stimulated GTP hydrolysis by the Rag GTPases. *J Biol Chem*. (2019) 294:2970–5. doi: 10.1074/jbc.AC119.007382
28. Pudakalakatti S, Titus M, Enriquez JS, Ramachandran S, Zacharias NM, Shureiqi I, et al. Identifying the metabolic signatures of PPAR δ -overexpressing gastric tumors. *Int J Mol Sci*. (2022) 23. doi: 10.3390/ijms23031645
29. Padua D, Pinto DF, Figueira P, Pereira CF, Almeida R, Mesquita P. HMGA1 has predictive value in response to chemotherapy in gastric cancer. *Curr Oncol*. (2021) 29:56–67. doi: 10.3390/curroncol29010005
30. Lin Y, Lin L, Fu F, Wang C, Hu A, Xie J, et al. Quantitative proteomics reveals stage-specific protein regulation of triple negative breast cancer. *Breast Cancer Res Treat*. (2021) 185:39–52. doi: 10.1007/s10549-020-05916-8
31. Terribas E, Fernandez M, Mazuelas H, Fernandez-Rodriguez J, Biayna J, Blanco I, et al. KIF11 and KIF15 mitotic kinesins are potential therapeutic vulnerabilities for Malignant peripheral nerve sheath tumors. *Neurooncol Adv*. (2020) 2:162–74. doi: 10.1093/noonadv/ndz061
32. Han J, Xie R, Yang Y, Chen D, Liu L, Wu J, et al. CENPA is one of the potential key genes associated with the proliferation and prognosis of ovarian cancer based on integrated bioinformatics analysis and regulated by MYBL2. *Transl Cancer Res*. (2021) 10:4076–86. doi: 10.21037/tcr-21-175
33. Feng Y, Li F, Yan J, Guo X, Wang F, Shi H, et al. Pan-cancer analysis and experiments with cell lines reveal that the slightly elevated expression of DLGAP5 is involved in clear cell renal cell carcinoma progression. *Life Sci*. (2021) 287:120056. doi: 10.1016/j.lfs.2021.120056
34. Ueda Y, Ooshio I, Fusamae Y, Kitae K, Kawaguchi M, Jingushi K, et al. AlkB homolog 3-mediated tRNA demethylation promotes protein synthesis in cancer cells. *Sci Rep*. (2017) 7:42271. doi: 10.1038/srep42271
35. Nakaya HI, Wrammert J, Lee EK, Racioppi L, Marie-Kunze S, Haining WN, et al. Systems biology of vaccination for seasonal influenza in humans. *Nat Immunol*. (2011) 12:786–95. doi: 10.1038/ni.2067
36. Sakai M, Shimokawa T, Kobayashi T, Matsushima S, Yamada Y, Nakamura Y, et al. Elevated expression of C10orf3 (chromosome 10 open reading frame 3) is involved in the growth of human colon tumor. *Oncogene*. (2006) 25:480–6. doi: 10.1038/sj.onc.1209051
37. Jeffery J, Sinha D, Srihari S, Kalimutho M, Khanna KK. Beyond cytokinesis: the emerging roles of CEP55 in tumorigenesis. *Oncogene*. (2016) 35:683–90. doi: 10.1038/onc.2015.128
38. Stelzer G, Rosen N, Plaschkes I, Zimmerman S, Twik M, Fishilevich S, et al. The GeneCards suite: from gene data mining to disease genome sequence analyses. *Curr Protoc Bioinf*. (2016) 54:1 30 1–1 3. doi: 10.1002/0471250953.2016.54.issue-1
39. Capece D, Verzella D, Fischietti M, Zazzeroni F, Alesse E. Targeting costimulatory molecules to improve antitumor immunity. *J BioMed Biotechnol*. (2012) 2012:926321. doi: 10.1155/2012/926321
40. Singh R, Kaul R, Kaul A, Khan K. A comparative review of HLA associations with hepatitis B and C viral infections across global populations. *World J Gastroenterol*. (2007) 13:1770–87. doi: 10.3748/wjg.v13.i12.1770
41. Tan L, Qin Y, Xie R, Xia T, Duan X, Peng L, et al. N6-methyladenosine-associated prognostic pseudogenes contribute to predicting immunotherapy benefits and therapeutic agents in head and neck squamous cell carcinoma. *Theranostics*. (2022) 12:7267–88. doi: 10.7150/thno.76689
42. Spurlock CF 3rd, Tossberg JT, Guo Y, Collier SP, Crooke PS 3rd, Aune TM. Expression and functions of long noncoding RNAs during human T helper cell differentiation. *Nat Commun*. (2015) 6:6932. doi: 10.1038/ncomms7932
43. Zhang C, Dang D, Cong L, Sun H, Cong X. Pivotal factors associated with the immunosuppressive tumor microenvironment and melanoma metastasis. *Cancer Med*. (2021) 10:4710–20. doi: 10.1002/cam4.v10.14
44. Zhang X, Weng C, Li Y, Wang X, Jiang C, Li X, et al. Human Bop is a novel BH3-only member of the Bcl-2 protein family. *Protein Cell*. (2012) 3:790–801. doi: 10.1007/s13238-012-2069-7
45. Smith DJ, Forrest S, Ackley DH, Perelson AS. Variable efficacy of repeated annual influenza vaccination. *Proc Natl Acad Sci U S A*. (1999) 96:14001–6. doi: 10.1073/pnas.96.24.14001
46. Caskey M, Lefebvre F, Filali-Mouhim A, Cameron MJ, Goulet JP, Haddad EK, et al. Synthetic double-stranded RNA induces innate immune responses similar to a live viral vaccine in humans. *J Exp Med*. (2011) 208:2357–66. doi: 10.1084/jem.20111171
47. Team H-CSP, Consortium H-I. Multicohort analysis reveals baseline transcriptional predictors of influenza vaccination responses. *Sci Immunol*. (2017) 2. doi: 10.1126/sciimmunol.aal4656
48. Fourati S, Tomalin LE, Mule MP, Chawla DG, Gerritsen B, Rychkov D, et al. Pan-vaccine analysis reveals innate immune endotypes predictive of antibody responses to vaccination. *Nat Immunol*. (2022) 23:1777–87. doi: 10.1038/s41590-022-01329-5
49. Tsang JS, Dobano C, VanDamme P, Moncunill G, Marchant A, Othman RB, et al. Improving vaccine-induced immunity: can baseline predict outcome? *Trends Immunol*. (2020) 41:457–65. doi: 10.1016/j.it.2020.04.001